ACS APPLIED POLYMER MATERIALS

pubs.acs.org/acsapm Article

Achieving Highly Conductive, Stretchable, and Washable Fabric from Reactive Silver Ink and Increased Interfacial Adhesion

Anthony J. Galante, Brady C. Pilsbury, Mingxuan Li, Melbs LeMieux, Qihan Liu, and Paul W. Leu*

Cite This: https://doi.org/10.1021/acsapm.2c00768 Read Online

ACCESS | Metrics & More | Article Recommendations | Supporting Information

ABSTRACT: There is a major need to manufacture highly electrically conductive fabrics with stretch- and wash-durability. In this work, we provide both modeling and experiments of the mechanical failure of silver ink coatings on knitted fabric. Large thickness metal films are needed for high conductance but tend to debond from the underlying fabric microfibers that lead to cracking and failure. Strong adhesion between the metal film and microfiber is thus key to achieving high thickness films with good mechanical robustness. The use of a reactive silver ink addresses this need due to in situ silver reduction and conformal coverage. Furthermore, a chemical etchant pretreatment of the textile microfibers functionalizes the surface to enable covalent bonding with the surface and increases theinterface area. The use of a polymer provides for an additional protective barrier during washing. Treated fabrics demonstrate low sheet resistance <100 mΩ per square with only two coats and <200 mΩ per square after 1000 stretching cycles or 300 min of ultrasonic washing with detergent.

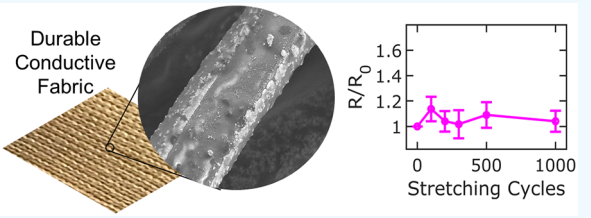

KEYWORDS: *conductive, fabric, e-textile, ink, durability, coating, adhesion, resistance*

INTRODUCTION

Flexible and electrically conductive fabrics are needed for a wide variety of applications such as wearable sensing, energy storage, electromagnetic shielding, wireless communication, and health monitoring.[1−5] However, it remains a challenge to demonstrate high conductance on fabrics and durability to maintain this high conductance after handling, general wear, stretching, and/or washing.[6] Previous strategies to achieve durable conductive fabrics have failed to achieve <1000 mΩ per square sheet resistance.[7−9] These strategies have utilized conductive polymers, metal salts, or integration of metal yarns, which do not demonstrate as high a conductance as coating pure metal films over fabric. Other works have achieved <1000 mΩ per square sheet resistance by using electroless metal deposition[10] or metal nanowire composites;[11] however, these studies have neglected to evaluate the degradation in sheet resistance after stretching and/or washing. Similarly, electroplating techniques have been utilized to create flexible conductors; however, these techniques have drawbacks such as slow throughput, high energy consumption, and high production of waste.[12,13] There is a need for simple fabrication methods to create high conductance fabrics with long lasting durability.

Techniques to achieve stretchable conductance using silver nanowires have been reported;[14,15] however, nanowires have drawbacks such as high roughness, low adhesion to surfaces, poor stability, and high contact resistance at wire junctions.[16] Inkjet printing of reactive silver inks for stretchable, washable conductive fabrics has also been reported; however, these works have required at least eight printing passes to achieve low (<1000 mΩ per square) sheet resistance.[17−19] Manufacturing stretchable conductors is mechanically challenging, as highly conductive metal films fracture at a few percent of strain.[20] Metal coatings over textile fiber can easily be cracked from repeated stretching or washing.[17,18,21]

In this work, we investigate the mechanical failure of silver coatings on knitted fabrics under stretching and washing loads. We derive a simple mechanical model that shows that enhancing the adhesion between the coating and the film and adding a protective barrier are key for durability under both types of loads. We demonstrate several strategies to achieve low sheet resistance and durability under both stretching and washing loads.

We utilize a reactive silver ink amine complex[22] to render a conductive property on polyethylene terephthalate (PET) knit fabric. PET knit fabric is common for garments because of its low cost, durability, comfort, and elasticity.[23] Knit fabric has a higher stretchability than most weaves. The reactive silver ink reduces in situ on the textile and uniformly covers the microfibers of the fabric. This provides for better electrical conductance and silver adhesion with the fabric microfibers

Received: May 6, 2022
Accepted: May 19, 2022

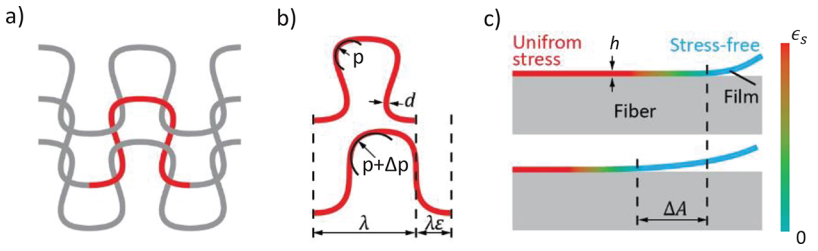

Figure 1. Modeling of films on knitted textiles. (a) Schematic of knitted textile consisting of loops of fibers. (b) Illustration of how a knitted fiber loop can accommodate large stretch through small bending strain. (c) Model of film debonding on the microfiber.

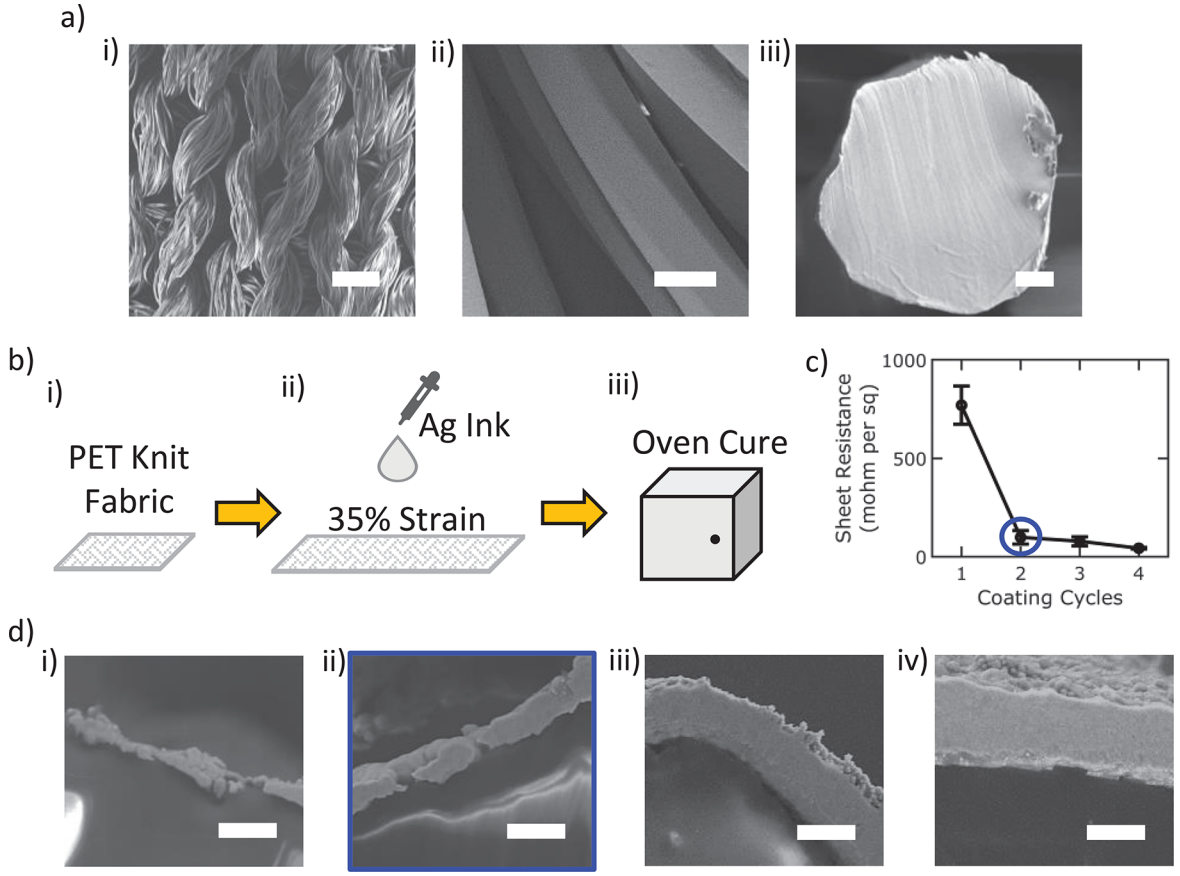

Figure 2. Coating of reactive silver ink on knit PET fabrics. (a) Representative SEM images of the size scale of knit PET fabric for order of magnitude estimations. Scale bars: (i) 200 μm, (ii) 9 μm, (iii) 2 μm. (b) Schematic of silver treatment on (i) PET fabric where (ii) fabric is stretched while drop casting silver ink followed by (iii) oven curing. (c) Sheet resistance as a function of coating cycles where the blue circle corresponds to PET-Ag samples. (d) Cross-sectional image of silver film thickness after (i) one, (ii) two, (iii) three, and (iv) four coating cycles. Scale bars: 700 nm. Additional experiments in this work evaluate samples coated with two coating cycles (PET-Ag, highlighted in blue).

than nanoparticles or nanowires. Highly electrically conductive microfibers are useful for electromagnetic shielding and extremely sensitive sensing applications.[11,24,25] The textiles are coated by a simple and efficient drop casting followed by oven curing; only a single coat of silver ink is necessary for sub Ω per square sheet resistance.

In addition to the use of a reactive metal ink, the metal adhesion to the underlying fiber is further improved by chemical etching. The etching process not only roughens the surface and increases the interface area, but also adds COO− groups that covalently bond to silver which greatly increase the adhesion energy to prevent debonding during stretching. Additionally, the coated fabric is further coated with PDMS on the outside to significantly improve the wash durability. The PDMS provides a protective barrier to prevent liquid infiltration from the detergent solution during washing. The combination of reactive silver inks, together with microfiber etching, and a barrier coating enables metal films that not only are highly conductive, but also have high durability under stretching and washing loads. Coated fabrics demonstrate <100 mΩ per square sheet with only two coats and exhibit <200 mΩ per square sheet resistance even after 1000 stretching cycles at 20% strain and 300 min of ulrasonic detergent washing.

RESULTS AND DISCUSSION

Section 1. Mechanical Analysis for Film Debonding.

We first develop a simple model for a silver film coated on a fiber under mechanical loads that occur during stretching and washing (Figure 1). Knitted textiles employ the bending of fibers to realize high stretchability.[26] The textile is shown

https://doi.org/10.1021/acsapm.2c00768
ACS Appl. Polym. Mater. XXXX, XXX, XXX−XXX

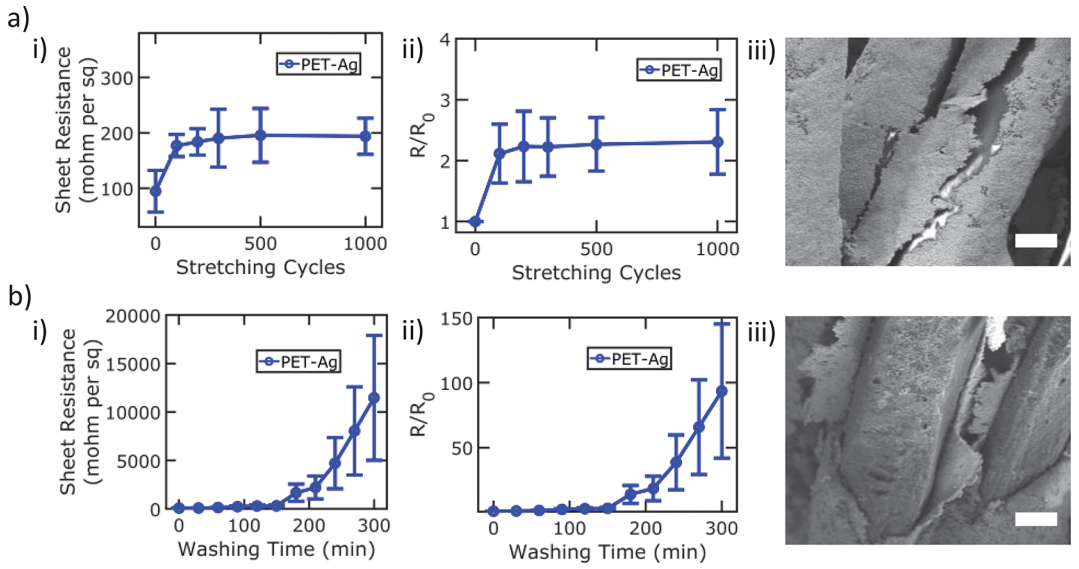

Figure 3. Durability performance of PET-Ag samples. (a) Stretching and (b) washing durability performance characterized by (i) sheet resistance, (ii) R/R_0, and (iii) representative SEM imaging. Scale bars: 5 μ m.

schematically in Figure 1a. The basic repeating unit in a knitted textile is a fiber loop. There could be many fibers in one loop if the fabric is knitted with yarns. The basic repeating unit is one single fiber in such a loop. When the textile is stretched, the curvature of the loop changes (Figure 1b). With the assumptions of Euler−Bernoulli beam theory,[27] the strain on the surface of the fiber, ϵ_s, is

$$\epsilon_s = \frac{d}{p} - \frac{d}{p + \Delta p} \tag{1}$$

where the radius of curvature of the loop is p, the diameter of the fiber is d, and Δp is the change of p because of deformation. If the overall strain applied is ϵ, then as a first order approximation $\Delta p \sim p\epsilon$. With a linear expansion of ϵ, we estimate

$$\epsilon_s \sim \frac{d}{p}\epsilon \tag{2}$$

ϵ_s is also the strain experienced by the silver coating during the stretching of the textile.

Locally, the debonding of the film from the fiber can be approximately modeled as a 2D problem because the film thickness is significantly less than the diameter of the fiber (Figure 1c). The debonded film is stress-free and uniformly stretched by ϵ_s deep inside the bonded region. Between the bonded and debonded region, there is a transition region of nonuniform stress. If the film debonds by area ΔA, the transition region moves, but the associated stress field does not change. The area of the stress-free region increases by ΔA, and the uniformly stretched region decreases by ΔA. The overall energy released is $E_f\epsilon_s^2\, h\Delta A/2$, where E_f is the modulus of the film and h is the thickness of the film.

Debonding occurs when the energy released is larger than the adhesion energy between the film and the fiber, $\Gamma_{ad}\Delta A$, where Γ_{ad} is the interfacial adhesion energy. The energy balance then gives the debonding criterion[28]

$$\Gamma_{ad} \le \frac{E_f\epsilon_s^2 h}{2} \tag{3}$$

which results in

$$h_c = \frac{2\Gamma_{ad}}{E_f\epsilon_s^2} \tag{4}$$

Here, h_c is the critical film thickness above where debonding occurs. Thicker silver films are more desirable to achieve lower sheet resistances. However, under the same synthesis procedure and stretching conditions, thicker silver films are more likely to debond. Thus, to realize larger silver thicknesses, Γ_{ad} must be increased. If the film debonds from the fiber, a defect will lead to stress-concentration that tears the film. In contrast, if the film is bonded to the fiber, the fiber limits deformation in the film and thus prevents crack propagation. Good adhesion between the film and the fiber is thus key for a mechanically robust coating.

Section 2. Coating Performance without Modification. Figure 2 characterizes the knit PET fabric, as well as the coating process and characterization of reactive metal films on the fabric. For the PET knit fabric studied, the radial loop size of the fabric R is about 200 μm and the diameter of indiviual fibers d is about 10 μm (Figure 2a). Reactive silver ink is used to coat PET knit fabric to create highly conductive textiles with good adhesion to the underlying microfibers. Figure 2b shows a schematic of the silver ink coating process. First, PET knit fabric (Figure 2bi) is stretched by a vice before coating to reduce the operable strain in the film during stretching. Then, 0.5 mL of silver ink is dropped onto the fabric (Figure 2bii) and samples are cured in an oven at 120 °C (Figure 2biii). This process is repeated for multiple coating cycles. The reactive silver ink reduces in situ on the textile microfibers and conformally covers the microfibers. The conformity of the silver ink provides a much larger contact area for better silver adhesion than silver nanoparticle and nanowire techniques.

Figure 2c shows the sheet resistance as a function of coating cycles. The sheet resistance decreases linearly with the number of coats after the first coat. In contrast, the sheet resistance is much higher after only just one coat, indicating that the initial film is not continuous. PET fabric samples are coated twice with silver (PET-Ag) to achieve a more continuous film and an average initial sheet resistance of $R_0 = 100 \pm 40$ mΩ per

https://doi.org/10.1021/acsapm.2c00768
ACS Appl. Polym. Mater. XXXX, XXX, XXX−XXX

square. The thickness of the silver ink coating after coating cycles is estimated by using cross-sectional SEM (Figure 2d). The estimated thickness is 350 ± 60 nm after two coats (Figure 2dii). Additional experiments are carried out on textile samples after two silver ink coating cycles (highlighted in blue) and the rest of the paper focuses on textiles coated with two cycles.

Figure 3 shows stretching and washing durability tests performed on textiles coated twice with silver ink. Stretching durability tests evaluate how the sheet resistance changes as a function of ϵ = 20% stretching cycles (Figure 3a). The sheet resistance increases to R = 190 ± 30 mΩ per square after 1000 stretching cycles (Figure 3ai) and R/R_0 increases to 2.3 ± 0.8 (Figure 3aii). PET-Ag exhibits increases in sheet resistance after stretching because of crack propagation and separation of the silver film. Cracks can be observed on the silver film by SEM (Figure 3aiii).

PET-Ag is also washed in detergent solution with ultrasonic agitation (Figure 3b). The ultrasonic cleaning procedure induces cavitation bubbles that produce high mechanical forces on the fabric,[29] which can play a dominant role in the removal of silver from fabrics.[30] The detergent solution additionally adds a chemical stress to the silver coating. The detergent is made of anionic surfactants and enzymes that stress the fabric coating by emulsification, lifting, and decomposition. The sheet resistance increases to 12500 ± 7600 mΩ per sq after 300 min of washing (Figure 3bi), and R/R_0 increases to 97.3 ± 42.8 (Figure 3bii). Removed layers of silver are observed on PET-Ag samples after ultrasonic washing. Entire layers of the silver film are ripped off from the microfibers of the fabric (Figure 3biii) because of strong mechanical forces induced during ultrasonic agitation in detergent solution.

Here, we analyze the experimental observation with an order-of-magnitude estimation based on the theory developed in Section 1. For a macroscopically applied stretch $\epsilon \sim 10\%$, eq 2 provides the strain on the coating, $\epsilon_s \sim 1\%$. Assuming the Young's modulus of sintered silver is $E_f \sim 100$ GPa[31] and the silver film thickness is $h_c \sim 100$ nm, by eq 4 the adhesion energy required to prevent debonding is $\Gamma_{ad} \sim 1$ J/m^2. In the absence of chemical bonding, the interfacial energy is often on the order of ∼0.1 J/m^2. Consequently, the observed large scale debonding is expected. According to eq 4, prevention of the debonding can be achieved by reducing the film thickness, h, or increasing the adhesion energy, Γ_{ad}. To prevent the film debonding at $\Gamma_{ad} \sim 0.1$ J/m^2, h must reduce by 1 order of magnitude, to $h \sim 10$ nm. Reducing the film thickness to about 10 nm will greatly increase the sheet resistance. Consequently, an effective way to increase Γ_{ad} is crucial to maintain low sheet resistance.

Section 3. Enhancing Adhesion. To improve the durability, we seek to increase the interfacial adhesion energy Γ_{ad} by chemically etching the microfiber surface with KOH and $KMnO_4$ to create etched PET (EPET) prior to ink deposition and curing. The etching process generates carboxyl groups on the fiber surface, which can form covalent bonding with the silver ink. The silver ink contains silver acetate compounds, which exchange silver ions from the carboxyl group of the acetate to the carboxyl groups on the PET microfibers to form covalent bonds.[22,32] The etching also increases the surface roughness, which further improves the adhesion energy (Figure 4).

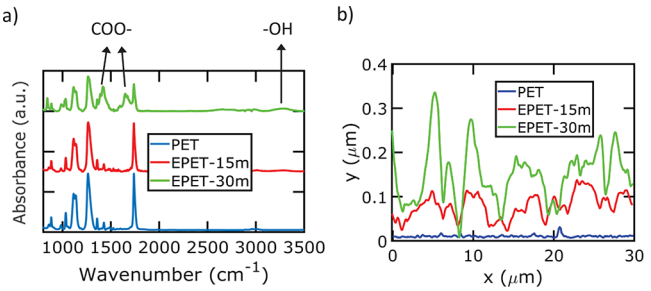

Figure 4. Chemical etching characterization of flat PET. (a) FTIR analysis of surface chemistry for flat PET after etching for 0, 15, and 30 min. (b) Root mean square roughness profile of samples for 0, 15, and 30 min etching taken by AFM.

The etching mechanism involves an oxidation and hydrolysis process.[33,34] The aliphatic carbons on the ethylenic group of PET are oxidized by $KMnO_4$, forming hydroxyl and carboxylate groups that increase the hydrophilicity. At the same time, the small chains of PET oligomer break down through hydrolysis reaction under a KOH environment, and thus the roughness is increased.[33,34] Fourier transform infrared (FTIR) spectroscopy only reveals new peaks after 30 min of chemical etching (Figure 4a). The new peaks are −OH bending at 1387−1426 cm^{-1}, −OH stretching at 3161−3300 cm^{-1}, C═O stretching at 1610−1550 cm^{-1}, C—O stretching at 1420−1300 cm^{-1}, and C—O bending at 1320−1211 cm^{-1}. The presence of COO− and −OH after 30 min of etching validate the oxidation of the PET surface. Most importantly, the surface chemical group COO− can form covalent bonds with reactive silver.[32] Covalent bonding generally has an interfacial energy on the order of 1 J/m^2.[35] The fabric etching process enables covalent bonding between the PET microfiber and the silver film to increase Γ_{ad} to the order of 1 J/m^2, which will be sufficient to prevent debonding according to the order of magnitude estimation in Section 2. Because bulk dissipation can dramatically enhance the adhesion energy when the interface is sufficiently strong, the true Γ_{ad} may be even higher.[36]

The increase in surface roughness from etching is portrayed by Figure 4b. The surface area increases as a function of etching time. The ratio of the surface area over projected area (30 × 30 μm^2) is estimated to be 1.02 by atomic force microscopy (AFM) prior to etching. After etching for 15 min, the ratio of surface area over projected area increases to 1.16. A significant increase in roughness is not observed until after 15 min of etching time where nanoscale roughness is observed. After etching for 30 min, the ratio of surface area over projected area further increases to 1.32. Larger submicron-sized pits are observed. Representative AFM scans are shown in Figure S1. The overall increase in total surface area over projected area from chemical etching after 30 min is 30%. Because Γ_{ad} is calculated for the projected area, this increase in real surface area is expected to increase Γ_{ad} by 30%. Surface energy and work of adhesion calculations suggest increases in the work of adhesion between the two interfaces from etching is on the scale of 0.1 J/m^2 (Figure S2), which is not enough to significantly improve debonding; therefore, we conclude the main cause of enhanced adhesion to the order of 1 J/m^2 is from covalent bonding and surface roughness.

Figure 5 demonstrates the physical morphology and performance of double-coated silver ink on etched PET fabric (EPET-Ag). Figure 5a shows SEM images of microfibers for

https://doi.org/10.1021/acsapm.2c00768
ACS Appl. Polym. Mater. XXXX, XXX, XXX−XXX

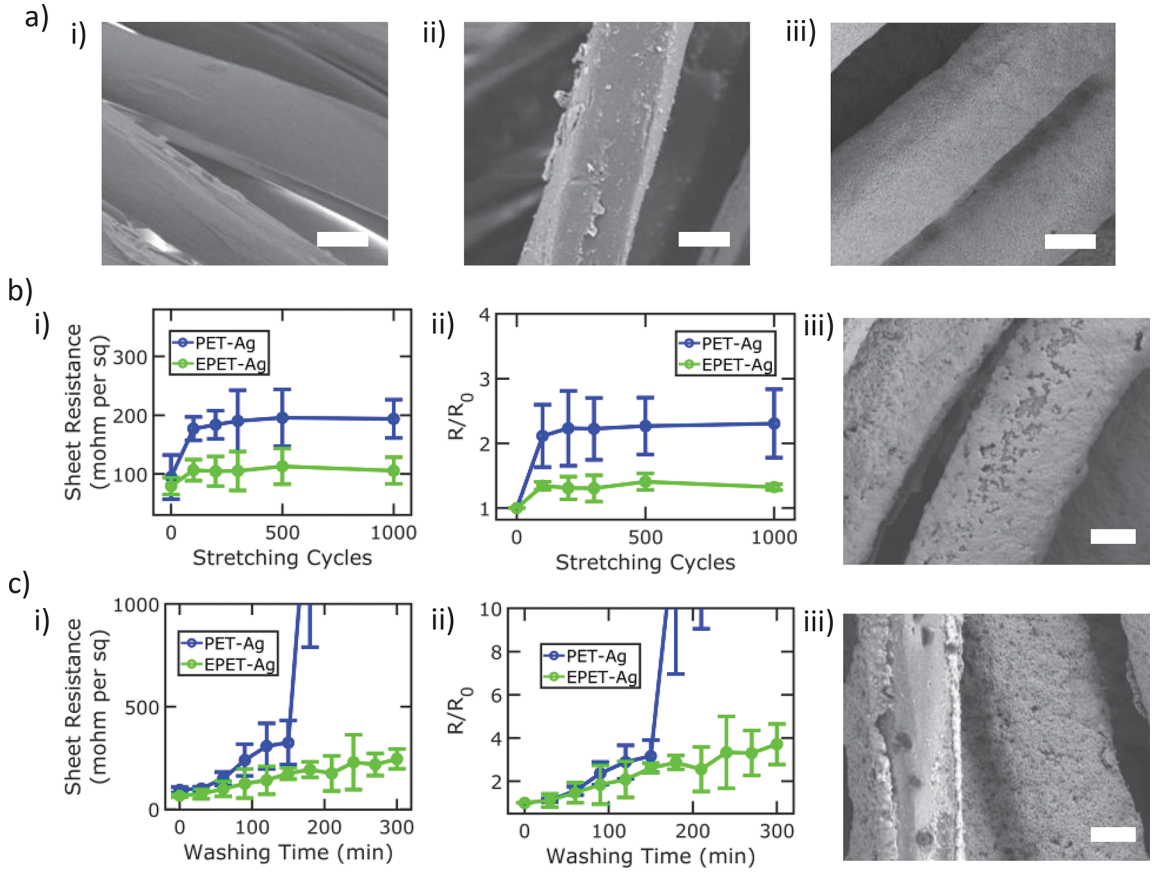

Figure 5. Characterization and performance of silver coating on etched PET (EPET-Ag) compared to results on PET (PET-Ag). (a) SEM images of treated fibers of (i) untreated PET, (ii) etched PET, and (iii) EPET-Ag. (b) Stretching durability and (c) washing durability performance of PET-Ag and EPET-Ag samples characterized by (i) sheet resistance, (ii) R/R_0, and (iii) representative SEM imaging. Scale bars: 5 μm.

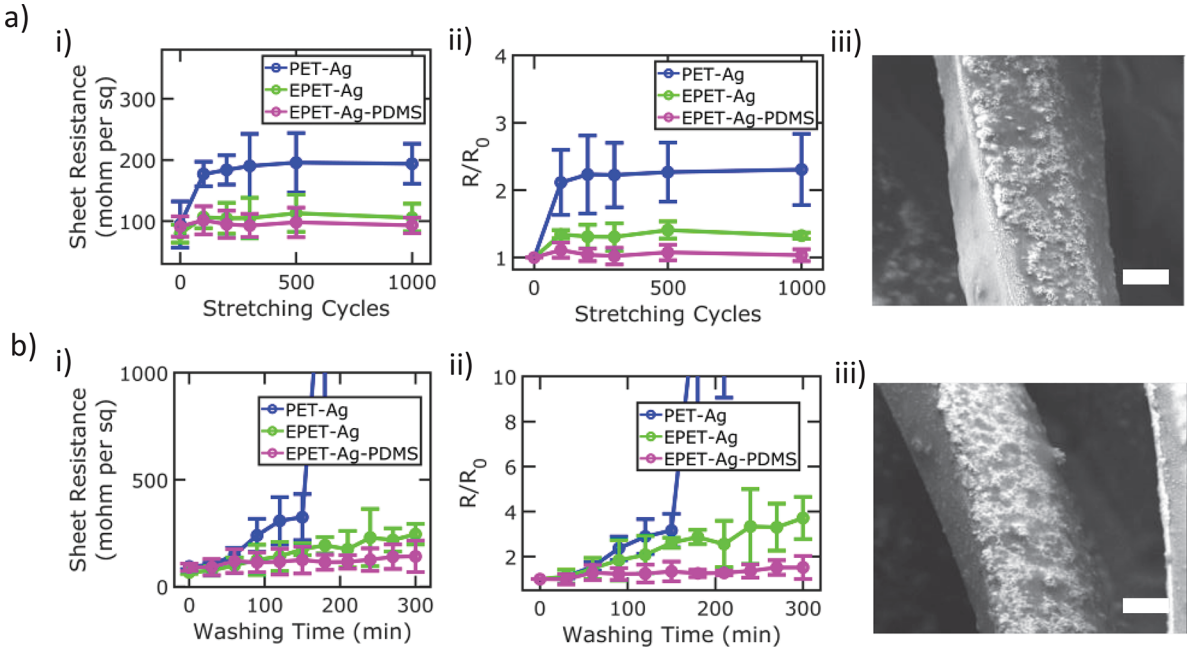

Figure 6. Characterization and durability performance of silver coated on etched PET followed by PDMS coating (EPET-Ag-PDMS), compared to the results with silver coated on etched PET (EPET-Ag) and silver coated on PET (PET-Ag). (a) Stretching and (b) washing durability performance comparison characterized by (i) sheet resistance, (ii) R/R_0, and (iii) representative SEM imaging. Scale bars: 5 μm.

(i) untreated PET, (ii) EPET, and (iii) EPET-Ag. The additional roughness on the microfibers after etching with KOH and $KMnO_4$ is observed (Figure 5aii). The cured silver film on a coated microfiber is shown in Figure 5aiii.

https://doi.org/10.1021/acsapm.2c00768
ACS Appl. Polym. Mater. XXXX, XXX, XXX−XXX

Figure 5b consists of EPET-Ag samples as a function of 20% stretching cycles. EPET-Ag has an initial sheet resistance of 80 ± 20 mΩ per sq that increases to 120 ± 20 mΩ per sq after 1000 stretching cycles (Figure 5bi). EPET-Ag samples show smaller changes in sheet resistance from the improved silver adhesion to the microfibers. R/R_0 increases to 1.4 ± 0.1 (Figure 5bii). EPET-Ag samples show smaller crack propagation from stretching compared to PET-Ag after 1000 stretching cycles (Figure 5biii). SEM images indicate small regions of coating loss, without large scale debonding or crack propagation.

Figure 5c shows changes in the sheet resistance of EPET-Ag as a function of ultrasonic washing time in detergent solution. The sheet resistance increases to 250 ± 50 mΩ per square after 300 min of washing (Figure 5ci). R/R_0 increases to 3.9 ± 0.4 (Figure 5cii). Some of the silver film is removed during washing, and the film looks less continuous after 300 min of ultrasonic washing (Figure 5ciii). The silver loss is more localized as opposed to large scale debonding or crack propagation because ultrasonic washing can induce local stress much higher than uniform stretching. The friction between a textile in a mechanical washer is expected to have a similar effect.

Section 4. Protective Coating for Washing Durability. According to our discussion in Section 1, a protective polymer barrier is required to further improve the washing durability. We additionally coat the silver-coated etched fabric with PDMS (EPET-Ag-PDMS). The PDMS coating distributes the localized washing load and prevents detergent solution from infiltrating and emulsifying the silver film, which lowers the stress on the silver film and silver−fiber interface to improve the washing durability. Liquid infiltration and emulsification significantly amplifies the exfoliative washing stress. The PDMS has much better liquid repellency than a film of cured silver ink, so the washing stress is significantly reduced (Figure S3). Furthermore, because PDMS can accommodate much larger deformation than silver, PDMS debonding from the silver during washing will not cause fracture, and physical adhesion can re-form after the load is removed.

Also, because of the softness of PDMS, its propensity for debonding under stretching load is extremely low. As an order of magnitude estimation, the modulus of PDMS is $E_f \sim 1$ MPa,[37] the thickness of the PDMS is h ∼ 1 μm. According to eq 4 the Γ_{ad} on the PDMS-Ag interface and the additional Γ_{ad} on the Ag-PET interface required to prevent debonding is as low as 0.1 mJ/m^2. Moreover, PDMS coating adds a polymer barrier that protects the silver film from environmental degradations. Although we used PDMS in our study, the same principle applies to other polymer coatings.

Figure 6 summarizes the performance of double-coated silver ink and PDMS on etched PET fabric (EPET-Ag-PDMS). The treated fiber is further coated with PDMS, estimated to be 1.0 ± 0.4 μm in thickness by using cross-sectional SEM. Figure 6a plots the sheet resistance as a function of 20% stretching cycles. EPET-Ag-PDMS has an initial sheet resistance of 90 ± 20 that increases to 94 ± 13 mΩ per square after 1000 stretching cycles (Figure 6ai). R/R_0 increases to 1.1 ± 0.2 (Figure 6aii). EPET-Ag-PDMS does not show significant degradation after 1000 stretching cycles (Figure 6aiii). The additional stretching durability compared to that of EPET-Ag samples is likely because of better resistance to the friction between fibers during stretching, which is neglected in our simple model.

Figure 6b plots the sheet resistance of EPET-Ag-PDMS samples as a function of ultrasonic detergent washing time. EPET-Ag-PDMS shows an increase in resistance from 90 ± 20 to 140 ± 70 mΩ per square after 300 min of ultrasonic washing (Figure 6bi). R/R_0 increases to 1.5 ± 0.5 (Figure 6bii). EPET-Ag-PDMS samples have the lowest increase in sheet resistance after washing because of the liquid repellency and protective barrier properties of the PDMS layer. The coating prevents detergent solution from emulsifying, lifting, and decomposing the silver film during washing, as well as acting as a buffer layer that distributes the localized surface load. The microfibers of EPET-Ag-PDMS samples do not show significant degradation after 300 min of ultrasonic detergent washing (Figure 6biii). Etched PET samples with silver and PDMS have lower overall sheet resistance than pristine PET samples with silver and PDMS after 300 min of washing because of the higher adhesion energy (Figure S4). Enhancing the adhesion between the silver and fiber interface (as we show by chemical etching) provides better overall performance than only coating the PET with silver and PDMS.

The simple film debonding model explains the relationship between interfacial adhesion energy, film thickness, and Young's modulus. Reducing the thickness of the metal film helps to prevent debonding; however, this change leads to higher sheet resistances. Thus, to achieve extremely low sheet resistances, the interfacial adhesion energy between the metal film and the fabric must be improved. Etching the fabric before adding the ink significantly increases the interfacial adhesion energy, which improves the overall durability of the conductive fabric. Coating the etched fabric with a barrier layer as the last step significantly reduces the localized stress on the metal film and adds liquid infiltration protection, which improves the washing durability of the conductive fabric. This work demonstrates how sub Ω sheet resistance can be achieved on knit fabric even after 1000 stretching cycles at 20% strain and 300 min of ultrasonic detergent washing.

CONCLUSION

A highly conductive knit fabric with stretching and ultrasonic washing durability is achieved by using reactive silver ink. Modeling and experimental evidence are used to explain the durability of the conductive knit fabrics. Durability for conductive fabrics can be improved by increasing the adhesion energy. Techniques are demonstrated to improve the durability of larger thickness metal films, such as covalent bonding, increasing the area of metal to fabric contact and adding a preservation layer to the outside of the film. Deposition of a conformal metal film with high interfacial adhesion energy with the fabric is key for durable conductive performance on knit fabric. This work provides insight on the fabrication of durable conductive fabrics for future e-textile applications.

EXPERIMENTAL SECTION

Materials. PET knit wipes were purchased from Anticon. Isopropyl alcohol (99.5%) was bought from VWR. KOH in water (45%), $KMnO_4$, hexane, and PDMS (Sylgard 184) were bought from Sigma-Aldrich. Reactive silver inks (710 series) were provided by Electroninks. Deionized water was used from a Millipore Academic A10 system with total organic carbon below 40 ppb. The detergent powder, Extran MN 01 Powder, was bought from EMD Chemicals.

Sample Fabrication. Rectangular samples (2 cm by 2 cm) were cut from PET fabric. All samples were rinsed with isopropyl alcohol to eliminate possible contaminants and allowed to dry at ambient temperature. PET fabric was etched in 100 mL of 45% KOH in water

https://doi.org/10.1021/acsapm.2c00768
ACS Appl. Polym. Mater. XXXX, XXX, XXX−XXX

for 30 min at 80 °C followed by 500 mg of $KMnO_4$ in 100 mL of water for 30 min at 80 °C to prepare etched PET (EPET). A 500 μL aliquot of reactive silver ink was drop cast onto untreated and etched fabrics at 35% stretch by vice followed by oven curing for 1 h at 120 °C for a single coat. PET fabrics were coated twice to make PET-Ag and EPET-Ag samples. Lastly, EPET-Ag-PDMS samples were prepared by dip coating EPET-Ag samples in 10 μL of PDMS (Sylgard 184) at 1:10 curing agent ratio diluted in 10 μL of hexane. EPET-Ag-PDMS samples were cured in an oven at 150°C for 3 h and allowed to continue curing at ambient temperature overnight. To investigate the change in surface roughness, chemistry and wetting behavior from the chemical etching process, flat PET samples were etched in the KOH solution followed by the $KMnO_4$ solution for 15 and 30 min.

Sample Characterization. The physical morphologies of samples were characterized by scanning electron microscopy (SEM, Zeiss Sigma 500 VP) at 5 kV and atomic force microscopy in tapping mode (AFM, Multimode SPM). Gwyddion software was used for calculating the ratio of surface area over projected surface area from AFM scans. For SEM imaging, all samples were sputter coated with 10 nm palladium by using a sputter coater (Denton). The chemical compositions of samples were characterized by Fourier transform infrared spectroscopy (FTIR, Bruker Vertex 70LS) between 600 and 3200 cm^{-1} wavelengths.

The Fowkes method was used to estimate the total surface free energy of samples with water and a purely dispersive liquid, diiodomethane. The independent dispersion and polar surface energy components for each sample group were calculated by using Young's and Dupre's definition of adhesion equations.[38,39] The apparent contact angles of the two test liquids were used to quantify Young's contact angles with the Wenzel equation. Then, Young's angles were used to calculate the polar and dispersive surface energy components. These quantities were summed for the overall surface free energy. The surface free energy values were used to quantify the work of adhesion. The work of adhesion is defined as the work required to separate two interfaces. An effective lower bound for the adhesion energy Γ_{ad} is estimated by using the work of adhesion equation $W_{ad} = \gamma_{PV} + \gamma_{SV} - \gamma_{PS}$, where γ_{PV} is the surface energy of the PET and γ_{SV} is the surface energy of the silver ink and $\gamma_{PS} = \gamma_{PV} + \gamma_{SV} - 2\sqrt{\gamma_{PV}\gamma_{SV}}$, assuming no bulk energy dissipation.[40]

Sheet resistance was measured by using the Van der Pauw nonuniform method as programmed on the B1500A Semiconductor Device Analyzer (Agilent Technologies). BNC to alligator clip cables connected the semiconductor device analyzer to four contact points on the textile sample. Three samples of each sample type were measured.

Durability Testing. Stretching of the textile samples was performed with a 5750 Linear Abraser (Taber Industries) and custom sample mount. Sheet resistance measurements were taken when the textile was at the 20% stretched position.

Washing cycles were performed by using a Powersonic P230 Ultrasonic Cleaner (Crest) under ASTM G131-96 standards for washing materials by ultrasonic techniques. A detergent solution with 0.24 g of Extran MN 01 powdered detergent and 150 mL of water was prepared and transferred to 10 mL Eppendorf tubes to create an efficient washing solution. Samples were submerged in detergent solution in Eppendorf tubes and ultrasonicated for 30 min at 80 W and 44 °C to complete one wash cycle. Afterward, samples were dried on a hot plate at 100 °C for 10 min or until fully dry.

■ ASSOCIATED CONTENT

Supporting Information

The Supporting Information is available free of charge at https://pubs.acs.org/doi/10.1021/acsapm.2c00768.

Roughness analysis of flat PET from chemical etching, wetting and surface energy analysis of flat PET from chemical etching, wetting analysis of silver ink on PET and PDMS on PET, sheet resistance as a function of washing time for PET-Ag-PDMS and EPET-Ag-PDMS samples (PDF)

■ AUTHOR INFORMATION

Corresponding Author

Paul W. Leu − *Department of Industrial Engineering, University of Pittsburgh, Pittsburgh, Pennsylvania 15261, United States; Department of Mechanical Engineering and Department of Chemical Engineering, University of Pittsburgh, Pittsburgh, Pennsylvania 15261, United States*; Email: pleu@pitt.edu

Authors

Anthony J. Galante − *Department of Industrial Engineering, University of Pittsburgh, Pittsburgh, Pennsylvania 15261, United States*; orcid.org/0000-0002-1227-6771

Brady C. Pilsbury − *Department of Industrial Engineering, University of Pittsburgh, Pittsburgh, Pennsylvania 15261, United States*

Mingxuan Li − *Department of Industrial Engineering, University of Pittsburgh, Pittsburgh, Pennsylvania 15261, United States*

Melbs LeMieux − *Electroninks Inc., Austin, Texas 78744, United States*

Qihan Liu − *Department of Mechanical Engineering, University of Pittsburgh, Pittsburgh, Pennsylvania 15261, United States*

Complete contact information is available at: https://pubs.acs.org/10.1021/acsapm.2c00768

Notes

The authors declare no competing financial interest.

■ ACKNOWLEDGMENTS

This work was supported in part by the National Science Foundation (No. ECCS 1552712). The authors thank Dr. Daniel Lamont for his characterization expertise.

■ REFERENCES

(1) Krifa, M. Electrically Conductive Textile Materials—Application in Flexible Sensors and Antennas. *Textiles* **2021**, *1*, 239−257.

(2) Liu, X.; Li, D.; Chen, X.; Lai, W.-Y.; Huang, W. Highly Transparent and Flexible All-Solid-State Supercapacitors Based on Ultralong Silver Nanowire Conductive Networks. *ACS Appl. Mater. Interfaces* **2018**, *10*, 32536−32542.

(3) Li, D.; Liu, X.; Chen, X.; Lai, W.-Y.; Huang, W. A Simple Strategy towards Highly Conductive Silver-Nanowire Inks for Screen-Printed Flexible Transparent Conductive Films and Wearable Energy-Storage Devices. *Adv. Mater. Technol.* **2019**, *4*, 1900196.

(4) Li, D.; Yang, S.; Chen, X.; Lai, W.-Y.; Huang, W. 3D Wearable Fabric-Based Micro-Supercapacitors with Ultra-High Areal Capacitance. *Adv. Funct. Mater.* **2021**, *31*, 2107484.

(5) Li, D.; Lai, W.-Y.; Zhang, Y.-Z.; Huang, W. Printable Transparent Conductive Films for Flexible Electronics. *Adv. Mater.* **2018**, *30*, 1704738.

(6) Cherenack, K.; van Pieterson, L. Smart textiles: Challenges and opportunities. *J. Appl. Phys.* **2012**, *112*, 091301.

(7) Mamun, M. A. A.; Islam, M. T.; Islam, M. M.; Sowrov, K.; Hossain, M. A.; Ahmed, D. M.; Shahariar, H. Scalable Process to Develop Durable Conductive Cotton Fabric. *Advanced Fiber Materials* **2020**, *2*, 291−301.

(8) Wu, B.; Zhang, B.; Wu, J.; Wang, Z.; Ma, H.; Yu, M.; Li, L.; Li, J. Electrical Switchability and Dry-Wash Durability of Conductive Textiles. *Sci. Rep.* **2015**, *5*, 11255.

(9) Pei, Z.; Xiong, X.; He, J.; Zhang, Y. Highly Stretchable and Durable Conductive Knitted Fabrics for the Skins of Soft Robots. *Soft Robotics* **2019**, *6*, 687−700.
(10) Li, X.; Li, Y.; Guan, T.; Xu, F.; Sun, J. Durable, Highly Electrically Conductive Cotton Fabrics with Healable Superamphiphobicity. *ACS Appl. Mater. Interfaces* **2018**, *10*, 12042−12050.
(11) Wang, Y.; Peng, S.; Zhu, S.; Wang, Y.; Qiang, Z.; Ye, C.; Liao, Y.; Zhu, M. Biomass-Derived, Highly Conductive Aqueous Inks for Superior Electromagnetic Interference Shielding, Joule Heating, and Strain Sensing. *ACS Appl. Mater. Interfaces* **2021**, *13*, 57930−57942.
(12) Reis, M. T. A.; Ismael, M. R. C. Electroplating wastes. *Physical Sciences Reviews* **2018**, *3*, 20180024.
(13) Rajoria, S.; Vashishtha, M.; Sangal, V. K. Review on the treatment of electroplating industry wastewater by electrochemical methods. *Materials Today: Proceedings* **2021**, *47*, 1472−1479. *Sustainable Technologies in Water Treatment and Desalination*; CRC Press, 2022; "Materials Science" (STWTD- 2020).
(14) Zhu, H.-W.; Gao, H.-L.; Zhao, H.-Y.; Ge, J.; Hu, B.-C.; Huang, J.; Yu, S.-H. Printable elastic silver nanowire-based conductor for washable electronic textiles. *Nano Research* **2020**, *13*, 2879−2884.
(15) Yao, S.; Yang, J.; Poblete, F. R.; Hu, X.; Zhu, Y. Multifunctional Electronic Textiles Using Silver Nanowire Composites. *ACS Appl. Mater. Interfaces* **2019**, *11*, 31028−31037.
(16) Azani, M.-R.; Hassanpour, A.; Torres, T. Benefits, Problems, and Solutions of Silver Nanowire Transparent Conductive Electrodes in Indium Tin Oxide (ITO)-Free Flexible Solar Cells. *Adv. Energy Mater.* **2020**, *10*, 2002536.
(17) Shahariar, H.; Kim, I.; Soewardiman, H.; Jur, J. S. Inkjet Printing of Reactive Silver Ink on Textiles. *ACS Appl. Mater. Interfaces* **2019**, *11*, 6208−6216.
(18) Kim, I.; Shahariar, H.; Ingram, W. F.; Zhou, Y.; Jur, J. S. Inkjet Process for Conductive Patterning on Textiles: Maintaining Inherent Stretchability and Breathability in Knit Structures. *Adv. Funct. Mater.* **2019**, *29*, 1807573.
(19) Stempien, Z.; Rybicki, E.; Rybicki, T.; Lesnikowski, J. Inkjet-printing deposition of silver electro-conductive layers on textile substrates at low sintering temperature by using an aqueous silver ions-containing ink for textronic applications. *Sens. Actuators, B* **2016**, *224*, 714−725.
(20) Pashley, D. W.; Bowden, F. P. A study of the deformation and fracture of single-crystal gold films of high strength inside an electron microscope. *Proceedings of the Royal Society of London. Series A. Mathematical and Physical Sciences* **1960**, *255* (1281), 218−231.
(21) Xu, B.; Eike, R. J.; Cliett, A.; Ni, L.; Cloud, R.; Li, Y. Durability testing of electronic textile surface resistivity and textile antenna performance. *Text. Res. J.* **2019**, *89*, 3708−3721.
(22) Walker, S. B.; Lewis, J. A. Reactive Silver Inks for Patterning High-Conductivity Features at Mild Temperatures. *J. Am. Chem. Soc.* **2012**, *134*, 1419−1421.
(23) Galante, A. J.; Yates, K. A.; Romanowski, E. G.; Shanks, R. M. Q.; Leu, P. W. Coal-Derived Functionalized Nano-Graphene Oxide for Bleach Washable, Durable Antiviral Fabric Coatings. *ACS Applied Nano Materials* **2022**, *5* (1), 718.
(24) Im, J. S.; Kang, S. C.; Lee, S.-H.; Lee, Y.-S. Improved gas sensing of electrospun carbon fibers based on pore structure, conductivity and surface modification. *Carbon* **2010**, *48*, 2573−2581.
(25) Choi, S.; Lee, H. M.; Kim, H. S. High performance and moisture stable humidity sensors based on polyvinylidene fluoride nanofibers by improving electric conductivity. *Polym. Eng. Sci.* **2019**, *59*, 304−310.
(26) Bueno, M.-A. In *Structure and Mechanics of Textile Fibre Assemblies*; Schwartz, P., Ed.; Woodhead Publishing Series in Textiles; Woodhead Publishing, 2008; pp 84−115.
(27) Gere, J. M.; Timoshenko, S. P. *Mechanics of materials*, 3rd ed.; PWS-KENT series in engineering; PWS-KENT Pub. Co.: Boston, 1990.
(28) Sun, J.-Y.; Lu, N.; Yoon, J.; Oh, K.-H.; Suo, Z.; Vlassak, J. J. Debonding and fracture of ceramic islands on polymer substrates. *J. Appl. Phys.* **2012**, *111*, 013517.
(29) Fuchs, F. J. In *Power Ultrasonics*; Gallego-Juárez, J. A., Graff, K. F., Eds.; Woodhead Publishing: Oxford, 2015; pp 577−609.
(30) Geranio, L.; Heuberger, M.; Nowack, B. The Behavior of Silver Nanotextiles during Washing. *Environ. Sci. Technol.* **2009**, *43*, 8113−8118.
(31) Walch, E. B. T.; Roos, C. Measurement of the mechanical properties of silver and enamel thick films using nanoindentation. *Int. J. Appl. Glass Sci.* **2020**, *11*, 195−206.
(32) Kapoor, S. Preparation, Characterization, and Surface Modification of Silver Particles. *Langmuir* **1998**, *14*, 1021−1025.
(33) Kim, S. J.; Bai, B. C.; Kim, M. I.; Lee, Y.-S. Improved specific capacitance of pitch-based activated carbon by KOH/KMnO4 agent for supercapacitors. *Carbon Letters* **2020**, *30*, 585−591.
(34) Mikhaylov, P. A.; Vinogradov, M. I.; Levin, I. S.; Shandryuk, G. A.; Lubenchenko, A. V.; Kulichikhin, V. G. Synthesis and characterization of polyethylene terephthalate-reduced graphene oxide composites. *IOP Conference Series: Materials Science and Engineering* **2019**, *693*, 012036.
(35) Tong, Q.-Y.; Fountain, G.; Enquist, P. Room temperature SiO2/SiO2 covalent bonding. *Appl. Phys. Lett.* **2006**, *89*, 042110.
(36) Liu, R.; Cui, L.; Wang, H.; Chen, Q.; Guan, Y.; Zhang, Y. Tough, Resilient, Adhesive, and Anti-Freezing Hydrogels Cross-Linked with a Macromolecular Cross-Linker for Wearable Strain Sensors. *ACS Appl. Mater. Interfaces* **2021**, *13*, 42052−42062.
(37) Johnston, I. D.; McCluskey, D. K.; Tan, C. K. L.; Tracey, M. C. Mechanical characterization of bulk Sylgard 184 for microfluidics and microengineering. *Journal of Micromechanics and Microengineering* **2014**, *24*, 035017.
(38) Fowkes, F. M. Attractive Forces at Interfaces. *Industrial & Engineering Chemistry* **1964**, *56*, 40−52.
(39) Galante, A. J.; Haghanifar, S.; Romanowski, E. G.; Shanks, R. M. Q.; Leu, P. W. Superhemophobic and Antivirofouling Coating for Mechanically Durable and Wash-Stable Medical Textiles. *ACS Appl. Mater. Interfaces* **2020**, *12*, 22120−22128.
(40) Butt, H.-J.; Graf, K.; Kappl, M. *Physics and Chemistry of Interfaces*; John Wiley & Sons, 2006; Google-Books-ID: zOD-c90UDk4sC.

https://doi.org/10.1021/acsapm.2c00768
ACS Appl. Polym. Mater. XXXX, XXX, XXX−XXX